Spiral Galaxies at z~1

© V.P. Reshetnikov [1,2]

[1] St.Petersburg State University, St.-Petersburg, Russia
[2] Email: vpresh@mail.ru

Abstract: We have conducted a systematic study of the surface brightness distribution for bright ($V_{606} \leq 23.5$) face-on ($b/a \geq$ . . 0.4) spiral galaxies at z~0.5-1. The sample was extracted from the HDF-N, HDF-S and HUDF and it consists of 117 spiral galaxies with available redshifts. Major and minor axes surface brightness profiles in the *I* band were investigated. In accordance with previous studies, we have found that most distant disks cannot be described by single exponential model. About 20-30% of galaxies demonstrate downbending profiles with mean break radius at 1.8 h_I (h_I - exponential scalelength of the inner disk). In agreement with Trujillo & Pohlen (2005), we have found that the break radius of distant galaxies correlates with their luminosity. From comparison of the correlations for local and distant galaxies, we confirm that radial position of the break radius evolve with redshift. This evolution is in qualitative agreement with results of numerical simulations for star-forming viscous disks under extended gaseous infall.

1. Introduction

Radial structure of stellar disks is an important test for galaxy formation models. It is well known that the surface brightness of the disks of nearby galaxies are well described by an exponential law (Patterson 1940). However, some stellar disks are truncated in the outer parts (van der Kruit 1979). Stellar disk truncations have been interpreted as a consequence of the suppression of star formation below a critical gas density. Also, van der Kruit (1987) has proposed that the truncation radius corresponds to the material with the highest specific angular momentum in the protogalaxy.

Pйrez (2004) demonstrated that it is possible to detect stellar disk truncations even at z~1. Trujillo & Pohlen (2005) used the position of the truncation as a direct estimator of the size of the stellar disk. After accounting for the surface brightness evolution of the galaxies, they found that the radial position of the truncations has increased with cosmic time by 1-3 kpc since z~1. Trujillo and Pohlen (2005) results give very simple and clear evidence in favour of inside-out growth of galactic disks. This conclusion is so important that we have decided to extend their analysis with the help of larger sample of distant galaxies and by using different method for the photometric profiles extraction.

Throughout, we adopt a flat cosmology with $Щ_m$=0.3, $Щ_Л$=0.7, and H_0=70 km /(s Mpc). All magnitudes are expressed in the AB system.

2. The sample

We have selected all objects with apparent magnitudes $V_{606} \leq . 23.^m5$ and axial ratios $b/a \geq . 0.4$ from three deep fields ─ HDF-N (Williams et al. 1996), HDF-S (Williams et al. 2000) and HUDF (Beckwith et al. 2006) ─ using publically available catalogues. In total, the sample included 201 object. We have excluded stars and objects near the frames margins.Then we have extracted the major and minor axes cuts in the *V* and *I* passbands and excluded all ellipticals and bulge-dominated galaxies from the sample. This leaves a total of 123 spiral galaxies. Spectroscopic redshifts for most of the HDF-N and HDF-S galaxies are from Cohen et al.(2000), Vanzella et al. (2002) and Sawicki & Mallйn-Ornelas (2003). For the HUDF galaxies we have used the COMBO-17 redshift estimates (Wolf et al. 2004). Final sample includes 117 spirals with z≤1.3.

3. Analysis

To investigate the surface brightness distribution, we have considered original major and minor axes cuts of the galaxies. We have used the public available F814W images with a scale of 0.04"/pixel for the HDF-N and HDF-S, and F775W mosaic for the HUDF (0.03"/pixel).

The profiles were averaged within 5x5 pixels (HDF-N and HDF-S) or within 3x3 pixels (HUDF). Such approach gives partly less deep photometric profiles in comparison with azimutal averaging (used by Pйrez 2004 and Trujillo & Pohlen 2005) but such profiles still suitable for the breaks/truncations searches. According to Pйrez (2004) and Trujillo & Pohlen (2005), distant galaxies often demonstrate relatively ``early'' and bright truncations/breaks and the detection limit м(I) ≈ 26-27 (approximately our limit) allows to detect such observational features with confidence.

From the other side, azimutal averaging includes in the final profile contributions from bars, star-formation regions and other non-axisymmetric features. Also, many distant galaxies look so asymmetric and peculiar that any significant smoothing can create false impression about surface brightness distribution. This add some systematics to the true shapes of the disks surface brightness distributions. So, it is important to check the dependence of the break radius on absolute magnitude using non-averaged galaxy profiles and with larger sample of galaxies.

3.1 Disk types

Following and Pohlen & Trujillo (2006) we have classified the profiles by three main classes: Type I (single exponential profile − with no systematic deviations from the exponent exceeding $0.^{m}5$), Type II (profile with downbending break), and Type III (upbending break) (see Fig. 1 for examples). Also, we have added Type IV class for strongly peculiar surface brightness distributions.

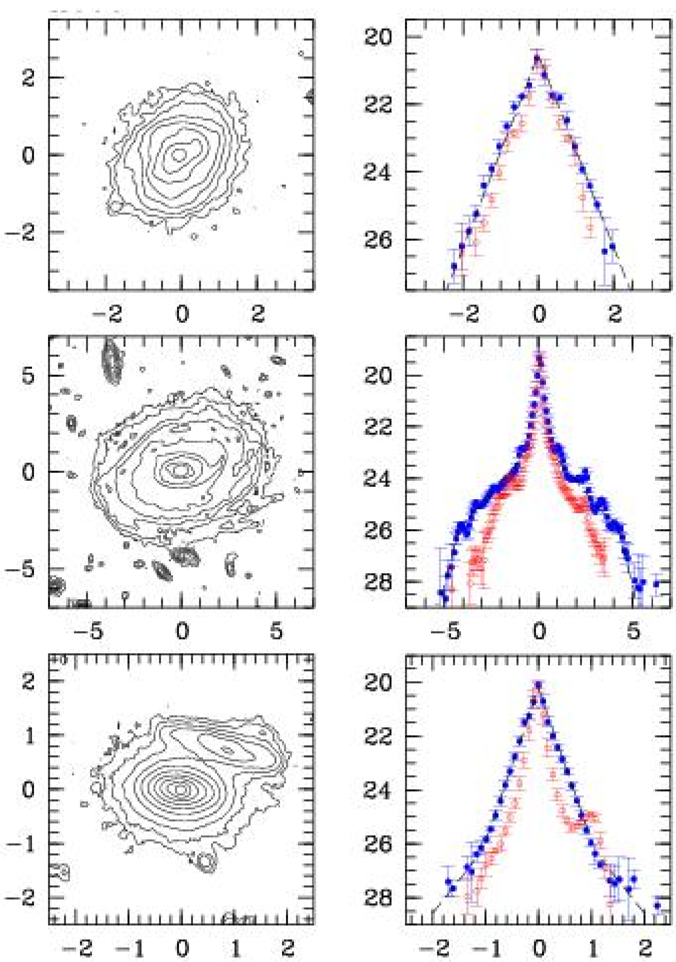

Fig. 1. *Left: I*-band contour plots (both axes are in arcsec), *right:* surface brightness profiles (in mag arcsec^2) of three galaxies. Solid circles show the major axes profiles, open circles — minor axes profiles. Dashed lines demonstrate exponential approximations of the data.

Top row — HDF-N galaxy 3-350.1 (Williams et al. 1996) with redshift 0.64 and Type 1 photometric profile.
Middle row — HUDF galaxy 423 (Beckwith et al. 2006) with z=0.47 and Type II profile (R_{br}=4."2).
Bottom row — HUDF galaxy 4584 (Beckwith et al. 2006) with z=0.64 and Type III profile (R_{br}=1."0).}

The position of the break radius (R_{br}) was determined by the same way as in Pohlen & Trujillo (2006). We have 7 joint with Trujillo & Pohlen (2005) Type II galaxies in the HUDF. The mean difference between our and T&P estimations of the R_{br} values is -0."04±0."24 (or around 3% only).

General characteristics of the sample (117 galaxies) are

$\langle M_B \rangle$ = -19.46 ±1.58 (mean absolute magnitude),
$\langle z \rangle$ = 0.53 ± 0.27 (mean redshift),
Type I frequency − 0.38 ± 0.06 (N=44),
Type II − 0.25 ± 0.05 (N=29),
Type III − 0.16 ± 0.04 (N=19),
Type IV − 0.21 ±0.04 (N=25).

Table 1 presents the parameters for bright ($L \geq L^*$) spirals only. As one can see, observational selection does not influence statistics of the profiles.

Table 1. Frequency of disk types for galaxies with $M_B \leq$ -19.5

	All	z ≤ 0.6	z > 0.6
Number	71	36	35
$\langle z \rangle$	0.65 ± 0.24	0.47 ± 0.09	0.84 ± 0.20
$\langle M_B \rangle$	-20.43 ± 0.69	-20.24 ± 0.65	-20.63 ± 0.68
Type I	0.42 ± 0.08 (N=30)	0.44 ± 0.11 (16)	0.40 ± 0.11 (14)
Type II	0.24 ± 0.06 (17)	0.28 ± 0.09 (10)	0.20 ± 0.08 (7)
Type III	0.14 ± 0.04 (10)	0.14 ± 0.06 (5)	0.14 ± 0.06 (5)
Type IV	0.20 ± 0.05 (14)	0.14 ± 0.06 (5)	0.26 ± 0.09 (9)

Our sample galaxies demonstrate expected evolution of the central surface brightness with redshift (Fig. 2, top). Exponential scalelengths of bright disks does not change with z (Fig. 2, bottom).

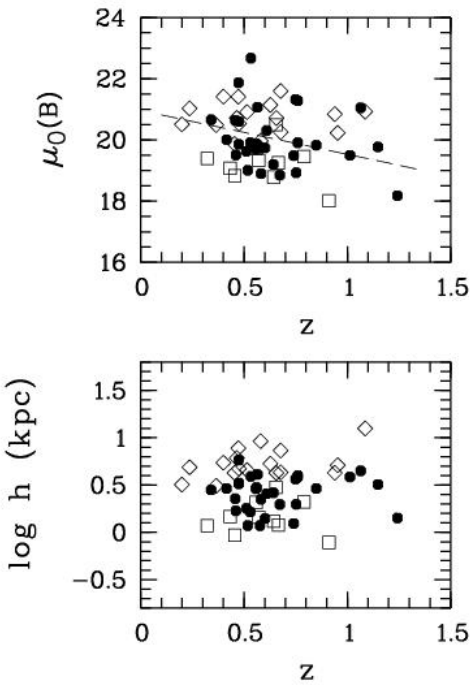

Fig. 2. Evolution of the rest-frame central surface brightness (top) and of the exponential scalelength (bottom) for bright ($M_B \leq$ -19.5) spiral galaxies in the HDF-N, HDF-S and HUDF. Filled circles show the data for pure exponential disks (Type I), rhombs − inner disks of galaxies with downbending profiles (Type II), and squares − inner disks of galaxies with upbending profiles (Type III). The dashed line corresponds to the surface brightness evolution for the GEMS disk galaxies (Barden et al. 2005).

The mean value of the R_{br} for the Type II galaxies is $(1.8 \pm 0.9)h_1$, where h_1 is exponential scalelength of the inner disk. This value is lower compared to samples of nearby spirals (see Pohlen & Trujillo 2006) and is consistent with Pйrez (2004) estimate for 6 z~1 galaxies. Corresponding value for the Type III galaxies is

(4.0 ± 1.0)h_1. The mean ratio of inner to outer scalelength is h_1 / h_2 = 2.8 ± 1.0 (Type II galaxies), for the Type III objects this ratio is 0.46 ± 0.15.

The mean values for the surface brightness at the break radius are μ(B) = 23.0 ± 1.2 (Type II) and μ(B) = 24.1 ± 1.1 (Type III) (in the rest-frame *B*-band). Both values are about one magnitude brighter in comparison with nearby galaxies (Pohlen & Trujillo 2006)

Fraction of Type IV profiles rises with redshift (Table 1). This rising approximately proportional to $(1+z)^{2.7}$ (assuming local fraction of such profiles as 0.05 − frequency of interacting and merging galaxies at z=0) and is in agreement with the observed evolution of the statistics of close pairs and mergers (e.g. Kartaltepe et al. 2007).

3.2 Bars frequence

We have tried to estimate bar fraction as a function of the profile type. Bars were identified by morphology based on contour plots and gray-scale images. In total, 27 galaxies can be classified as barred. The observed fraction of bars is, therefore, 0.23 ± 0.04. This is in good agreement with Elmegreen et al. (2004) statistics for spirals out to z=1.1 (0.23 ± 0.04).

The bar fraction according to galaxy types are

Type I − 0.20 ± 0.07 (N=9),
Type II − 0.34 ± 0.11 (N=10),
Type III − 0.16 ± 0.09 (N=3),
Type IV − 0.20 ± 0.09 (N=5).

The same distribution for bright galaxies ($M_B \leq$ -19.5) at z ≤ 0.6 is

all − 0.36 ± 0.10 (N=13),
Type I − 0.31 ± 0.14 (N=5),
Type II − 0.50 ± 0.22 (N=5),
Type III − 0.20 ± 0.20 (N=1),
Type IV − 0.40 ± 0.28 (N=2).

Therefore, observational selection undoubtedly influences the distributions. Within limits of poor statistics we can conclude only that bars present in galaxies with any types of surface brightness distribution (even with purely exponential distribution). To obtain any statistically significant conclusions we must enlarge the sample to a great extent.

4. Discussion

Using imaging data from three deep fields (HDF-N, HDF-S, HUDF), we have studied radial surface brightness distribution of a complete magnitude-limited sample of face-on distant spiral galaxies. We confirm earlier results that purely exponential stellar disks does not dominate among distant galaxies (e.g. Reshetnikov et al. 2003, Pйrez 2004, Trujillo & Pohlen 2005). Also, we found large fraction (~1/4 of all galaxies) of disks with downbending outer regions. The derived fraction is smaller in comparison with Trujillo & Pohlen (2005) (21/36 ≈ 60% for distant spirals) and Pohlen & Trujillo (2006) (≈ 60% for nearby galaxies) results, but relatively close to Pйrez (2004) (6/16 ≈ 40% for z~1 objects) ones. The difference in observed fractions can be attributed to different methods for profile extraction (azimutal averaging or major and minor axes cuts) and to a small number statistics. Also, we excluded most peculiar profiles from our analysis (Type IV in Sect. 3.1). Azimutal smoothing can ascribe such distributions to I − III types.

Fig. 3 presents ``the rest-frame absolute magnitude − the break radius'' relation for our distant galaxy sample. As one can see, the relation for our distant galaxies (Fig. 3, top) is in good agreement with average dependence according to Trujillo & Pohlen (2005) (dotted line). After the magnitude correction, the distant disks distribution moves closer to the local dependence (solid line) but stays well away from it (Fig. 3, bottom). Therefore, the break radius evolve with redshift − distant galaxies demonstrate systematically smaller R_{br} values. (This fact is in accord with our previous conclusion that stellar warps in z~1 disks appear to begin at a smaller radius − Reshetnikov et al. 2002.)

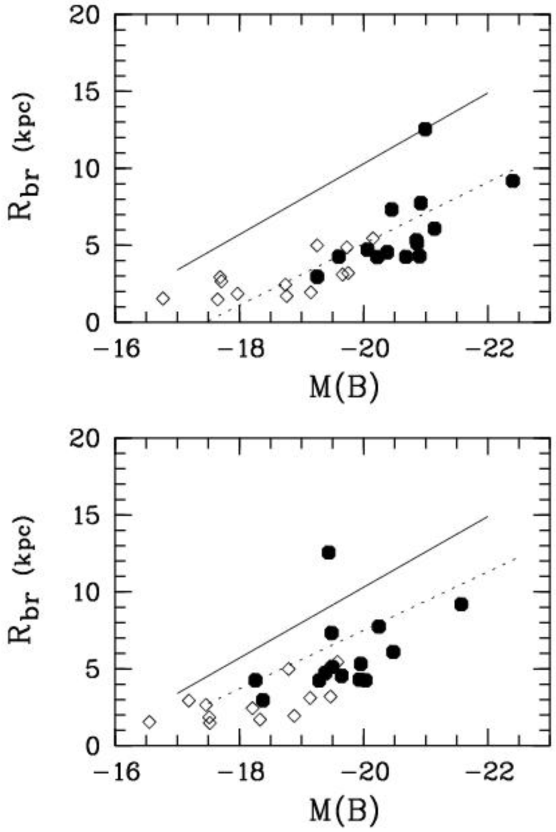

Fig. 3. *Top:* observed relation between the truncation radius and absolute magnitude in the rest-frame *B* band for the Type II disks. Filled circles − galaxies with $z \geq 0.45$, rhombs − $z < 0.45$ galaxies. *Bottom:* the same relation after correcting M_B values for the luminosity evolution (Barden et al. 2005). Solid line represent the local relation according to Trujillo and Pohlen (2005), dotted lines − relations for distant spirals from the same work.

Ferguson & Clarke (2001) presented numerical models of spiral galaxies which include simultaneous star formation, viscous redistribution of gas and cosmologically-motivated gaseous infall. Their Fig. 5 (middle row) shows clear evolution of the break radius with time for the extreme infall model. Therefore, the observed evolution of the break radius is in qualitative agreement with results of numerical simulations for star-forming viscous disks under extended gaseous infall.

I acknowledges partial financial support from the Russian Foundation for Basic Research (grant 06-02-16459).

References

1. Barden M., Rix H.-W., Somerville R.S. et al // ApJ. 635, 959 (2005).
2. Beckwith S.V., Stiavelli M., Koekemoer,A.M. et al // AJ. 132, 1729 (2006).
3. Cohen J.G., Hogg D.W., Blandford R. et al // ApJ. 538, 29 (2000).
4. Elmegreen B.G., Elmegreen D.M., Hirst A.C. // ApJ. 612, 191 (2004).
5. Ferguson A.M.N., Clarke C.J. // MNRAS. 325, 781 (2001).
6. Kartaltepe J.S., Sanders D.B., Scoville N.Z. et al // ApJS. 172, 320 (2007).
7. Patterson F.S. // Harvard Bull. 914, 9 (1940).
8. Pйrez I. // A&A. 427, L17 (2004).
9. Pohlen M., Trujillo I. // A&A. 454, 759 (2006).
10. Reshetnikov V., Battaner E., Combes F., Jimйnez-Vicente J. // A&A. 382, 513 (2002).
11. Reshetnikov V.P., Dettmar R.-J., Combes F. // A&A. 399, 879 (2003).
12. Sawicki M., Mallйn-Ornelas G. // AJ. 126, 2003 (2003).
13. Trujillo I., Pohlen M. // ApJ. 630, L17 (2005).
14. van der Kruit P.C. // A&AS. 38, 15 (1979).
15. van der Kruit P.C. // A&A. 173, 59 (1987).
16. Vanzella E., Cristiani S., Arnouts S. et al // A&A. 396, 847 (2002).
17. Williams R.E., Blacker B., Dickinson M. et al // AJ. 112, 1335 (1996).
18. Williams R.E., Baum S., Bergeron L.E., et al // AJ. 120, 2735 (2000).
19. Wolf C., Meisenheimer K., Kleinheinrich M. et al // A&A. 421, 913 (2004).